
ECR: MANIFOLD-GUIDED SEMANTIC CUES FOR COMPACT LANGUAGE MODELS

A PREPRINT

Chung-Wei (Victor) Yuan
YVIC Research Lab
 victor@yvic.dev

ABSTRACT

Compact models often lose the structure of their embedding space. The issue shows up when the capacity is tight or the data spans several languages. Such collapse makes it difficult for downstream tasks to build on the resulting representation. Existing compression methods focus on aligning model outputs at a superficial level but fail to preserve the underlying manifold structure. This mismatch often leads to semantic drift in the compact model, causing both task behavior and linguistic properties to deviate from the reference model. To address those issues, we provide a new framework called Embedding Consistency Regulation (ECR). This framework first derives a set of semantic anchors from teacher embeddings (computed once offline). Then, the compact model learns to maintain consistent geometry around these anchors, without relying on matching logits or internal features. ECR adds only a small projection step at inference, without altering the decoding architecture or its runtime behavior.

In experiments on a 100K multilingual corpus, ECR consistently stabilizes training and preserves semantic structure across tasks and languages. It also produces a more compact and task-aligned representation space, enabling low-capacity models to learn cleaner manifolds than conventional baselines. ECR works without teacher outputs and is compatible with, but independent of, distillation. Taken together, our results show that ECR helps compact models better follow task requirements and makes them easier to deploy under strict efficiency or privacy limits.

Keywords Representation learning • Model compression • Compact language models • Manifold • On-device AI

1 Introduction

More applications process sensitive information locally rather than sending it to the cloud [1]. Privacy regulations such as GDPR further restrict how user information may be transmitted [2]. The growing emphasis on privacy in modern machine learning systems has also been highlighted in recent surveys [3]. Compact models are often the only practical option when computation must remain local [4]. However, the limited memory and compute on edge hardware make it difficult for them to preserve the manifold structure of large models [5, 6].

Many existing compression methods focus on matching output behavior at the logit level rather than preserving internal semantic structure. [7, 8, 9]. As a result, a compact model may approximate the teacher’s outputs yet still lose the deeper task-related structure that organizes meaning.

When the gap in capacity is large, these shifts become stronger. After compression, the embedding space can lose its structure. Language regions that were well separated start to blur, and nearby clusters begin to interfere. Prior studies report similar forms of representation drift and semantic region overlap [10, 11].

These observations point to a structural rather than purely optimization-related problem. Classical work in PDP [12] and representation learning [13, 14] treats meaning as geometric structure distributed across representations. Such structure ideally remains stable under dimensionality reduction [15, 16, 17, 18]. Yet compact models often fail to maintain it, consistent with earlier observations on how aggressive compression affects representation quality.

Taken together, these results indicate that effective compact training should retain the structural regularities that support downstream tasks, not just match output behavior.

With ECR, the compact model maintains more consistent downstream behavior, instead of only imitating surface-level responses. During supervised fine-tuning, our method stabilizes the semantic patterns that normally drift in compact models, preventing the meanings and task from blending together. The result is a compact representation that remains stable enough for small task- or language-specific modules to plug into.

Across English, Chinese, and Hindi, the compact model behaves more predictably when trained with ECR. The cross-language shifts that normally happen in compact models are noticeably reduced. In several cases, the 1B FP32 model trained with our method surpasses the 3B baseline on targeted semantic tasks, even though the 1B model cannot match the 3B model in general-purpose settings. This suggests that the key difficulty in compact training is preserving the structure of the representation rather than the optimization process itself. ECR improves compact-model geometry without modifying the supervised loss or the model architecture, and without requiring extra teacher forward passes beyond the baseline KD setup.

Although ECR uses teacher embeddings once to build the anchors, it is not a teacher–student setup and does not perform distillation. No teacher logits, hidden states, or feature matching are used during training. The method works only through input-side conditioning, making it compatible with standard KD methods rather than a replacement for them.

Contributions.

- We show that the main difficulty in compact multilingual training comes from losing the teacher’s semantic organization after compression.
- We propose **ECR**, which adds a simple task-semantic signal to keep the compact model’s embedding space from drifting during training.
- We describe two variants—one retrieval-free and one retrieval-guided—so the method can fit different training setups.
- Experiments on English, Chinese, and Hindi show that ECR makes the compact model more stable and reduces cross-language drift. On several semantic tasks, the 1B FP32 compact model trained with ECR outperforms a 3B baseline.

To validate that the system works end to end, we deployed the distilled Luna-0.6B model on an iPhone 14. It includes local RAG retrieval, HNSW node visits during ef-search, the PCA (768→64) Metal kernel, cosine similarity computation, quantized decoding, and the corresponding GPU scheduling events. These traces confirm that the entire ECR pipeline executes fully on-device, without any remote calls.

2 Related Works

Prior work on compact models spans four main areas. These include distillation, representation geometry, retrieval-based modeling, and reasoning control. Each area addresses a different aspect of model behavior, and they are rarely integrated. Distillation typically aligns outputs or hidden states. Geometry work characterizes the structure of learned representations but seldom treats it as a trainable signal. Retrieval methods add external information, but they do not influence how the model structures its embedding space. Reasoning-control techniques influence model behavior but operate independently of its internal geometry.

We are not aware of prior work that uses retrieval signals to directly shape the geometric structure of compact models during training. ECR bridges these areas by turning teacher-side manifold information into an input-level control signal.

2.1 Distillation for Language Models

Most teacher–student compression setups supervise the student mainly through the teacher’s output logits [19, 8, 9, 20].

Some methods also try to match intermediate features instead of relying only on the final layer. For transformer LLMs, this idea has been extended to hidden states and even attention patterns [21].

These approaches usually assume that the teacher and student share a similar embedding space. The assumption becomes unreliable once the student is small or multilingual. Matching logits or hidden states does not ensure that the underlying geometry stays intact. Local neighborhoods may still change, and cross-lingual structure can shift even if the losses match.

Several recent works address this by adding geometric structure into the distillation process. A few works add contrastive pressure to the features, while others try to keep part of the teacher’s manifold during transfer [22, 23].

In all experiments, the compact model is trained using a standard KD loss. We compare KD alone with KD combined with ECR. ECR leaves the teacher loss unchanged. The anchors derived from the teacher serve only as a fixed geometric reference.

The objective stays the same under ECR. The student simply receives geometric signals through an additional, lightweight input-side cue. This control signal provides a small amount of geometric guidance without altering the original loss.

2.2 Representation Geometry

Manifold learning provides tools for examining how neural representations are organized. These methods often reveal smoother, low-dimensional patterns hiding inside high-dimensional embeddings [16, 15, 17]. Empirical studies in vision and language models highlight the role of geometric factors. Local geometric properties, variations in neighborhood

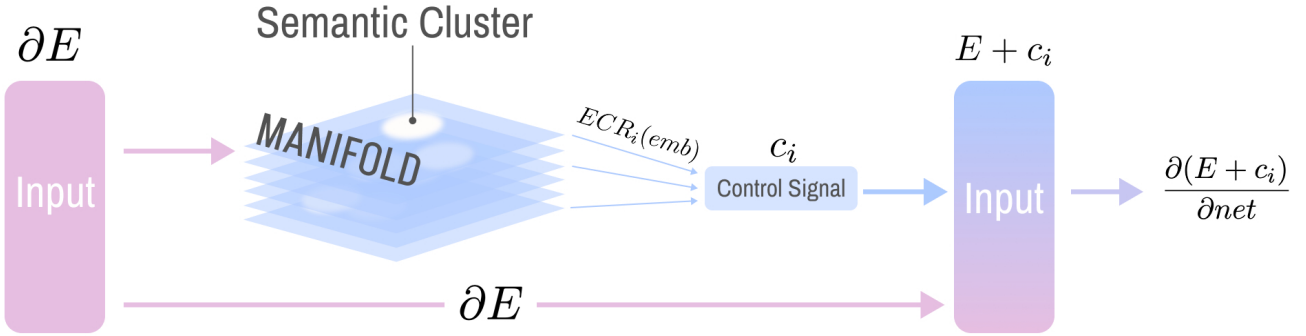


Figure 1: **Illustration of Embedding Consistency Regulation (ECR).** A query embedding is projected onto semantic manifold anchors through \mathcal{P}_i , yielding a discretized control signal c_i . These control codes are converted into prefix control tokens and inserted at the input layer, providing geometric cues that encourage the compact model to maintain more stable semantic organization during training. ECR operates *entirely through input conditioning*—no auxiliary losses, feature matching, or architectural modification are required. *The symbolic gradient notation is used only to illustrate the indirect effect that changed inputs have on the optimization trajectory; ECR does not modify gradients explicitly.*

structure, and interactions across domains all affect transferability and generalization [13, 18].

Several methods aim to capture geometric relations in embedding spaces [14, 22, 23, 11]. These include contrastive predictive coding, metric-preserving distillation, and multi-sense embedding alignment. These techniques help maintain local structure during learning.

ECR takes a different route. It does not enforce geometry through losses or feature matching. Instead, it brings manifold information in through the input. Teacher submanifolds are summarized as a small set of anchors. Their coordinates are turned into discrete control tokens. During training, these tokens nudge the small model toward a more consistent structure without changing the original objective.

2.3 Retrieval-Based Signals

Retrieval-augmented generation (RAG) [24, 25, 26] rely on an external search step that supplies additional context to the model. Token predictions are then conditioned on both the original input and the retrieved evidence. These methods guide the model using extra context or output-level cues, not by engaging with its internal geometry. ECR takes a different approach. It uses nearest-neighbor search to find which part of the teacher’s space the sample belongs to. That location is then turned into an internal geometric cue instead of extra context.

2.4 Reasoning and Control Mechanisms

Chain-of-thought (CoT) prompting helps with multi-step reasoning [27, 28]. Its stability, however, typically depends on long prompts and large models [29]. Other control mechanisms include task tokens [30], prefix-based conditioning [31], and lightweight modulation layers. These methods alter model behavior but preserve the underlying training objective.

However, these forms of control operate independently of the model’s representation geometry. They guide the model’s behavior, but they operate independently of its internal representation structure. Retrieved information and internal geometry remain loosely connected.

ECR integrates control with geometric structure. Coordinates derived from teacher clustering or retrieval are converted into internal control tokens. These tokens guide the optimization process and stabilize routing. They do so without relying on prompts or long CoT sequences. This makes ECR a good fit for compact on-device models, where prompt overhead is expensive.

3 ECR: Embedding Consistency Regulation

Compact language models often lose the stable semantic geometry preserved in their larger teachers. Regions that are cleanly structured in the teacher can collapse or bleed into one another after compression. Our goal is to stabilize this geometry without changing the supervised objective.

Instead of adding auxiliary losses or matching hidden states, ECR routes geometric information through the input. It reads an intermediate representation, maps it to a small discrete code, and feeds the code back as control tokens. The model is never asked to match teacher logits or features; it only receives a lightweight hint about where the example falls on the teacher manifold.

We begin with how limited capacity affects geometry, then outline the projection, discretization, and training pipeline. Two variants and their computational cost are discussed at the end.

3.1 Motivation: Geometry Under Capacity Constraints

Let $h \in \mathbb{R}^d$ be an intermediate representation and \mathcal{L} the supervised loss. Following the classical backprop view [32],

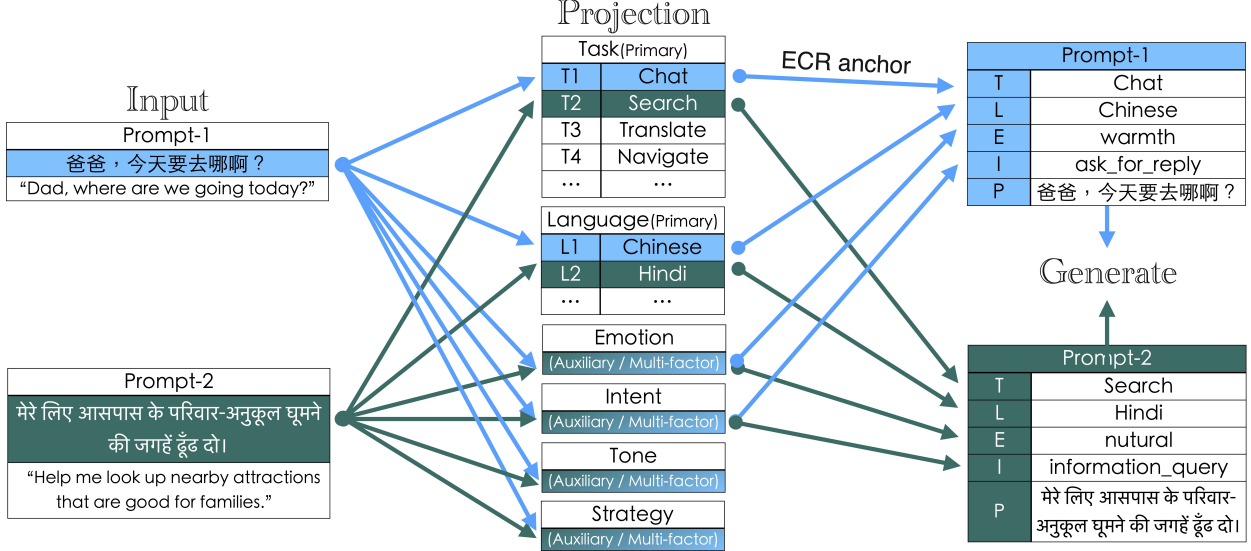


Figure 2: **Semantic factorization and control-token construction in ECR.** Each input query (left) is projected onto a structured semantic manifold consisting of primary factors (task, language) and multiple auxiliary dimensions (emotion, intent, tone, strategy). The projection identifies the closest semantic anchors, which are discretized into factor-specific control codes (T, L, E, I, P). These codes are emitted as prefix control tokens (right), forming an interpretable, factor-aligned conditioning signal that guides the compact model during generation. This figure illustrates two examples (Chinese and Hindi queries), showing that ECR handles multilingual and multi-factor semantics through the same projection–prefix pipeline.

updates to a weight matrix W take the form:

$$\Delta W = -\eta \frac{\partial \mathcal{L}}{\partial h} \frac{\partial h}{\partial W}.$$

This expression assumes the representation behaves reasonably well. It should be smooth in local areas and separate different semantic regions clearly. In compact or multilingual models, this structure often breaks down. Regions that should remain distinct start to merge; the space bends unevenly; boundaries that are clear in the teacher blur after compression.

These effects arise even when the loss function and optimizer remain unchanged. Once the geometry shifts, gradients move differently and training becomes less stable.

One way to address this is to add geometry-aware penalties. But this would require differentiable routing and Jacobian terms, which are not practical for compact models.

ECR keeps the loss intact and supplies geometric cues through the input instead. A small discrete code indicates the teacher region an example belongs to. Over time, the model learns to use this cue to organize its own representation space more consistently. The regularization happens through input conditioning rather than through an explicit geometric loss. **Clarification.** ECR is not a form of knowledge distillation. The teacher model is used only once to derive a fixed set of anchors; no teacher forward pass, logits, hidden states, or distillation loss is involved during training.

3.2 Problem Formulation

Teacher embeddings are first clustered into K groups, producing anchor vectors

$$\{\mu_k\}_{k=1}^K, \quad \mu_k \in \mathbb{R}^d.$$

These anchors form a fixed coordinate system derived entirely from the teacher model.

Given an input sequence x , the compact model computes an intermediate representation

$$h = f_\theta^{(\text{emb})}(x) \in \mathbb{R}^d.$$

Although h comes from the compact model, its location is evaluated relative to the teacher anchors.

After projecting h and discretizing the result, we obtain a short code:

$$t = \text{disc}(\mathcal{P}(h)), \quad t = [t_1, \dots, t_K], \quad t_i \in \{0, \dots, B-1\}.$$

This token prefix is prepended to the input:

$$x' = [t, x].$$

Training proceeds with the standard supervised objective

$$L(\theta) = \mathcal{L}(x'; \theta).$$

Thus, the only geometric signal comes from the teacher-derived prefix, not from teacher–student feature matching or auxiliary losses.

3.3 Semantic Projection Operator

Both h and the anchors μ_k are normalized:

$$\tilde{h} = h/\|h\|, \quad \tilde{\mu}_k = \mu_k/\|\mu_k\|.$$

The projection operator maps $h \in \mathbb{R}^d$ to a K -dimensional affinity vector:

$$\mathcal{P}(h) = [\cos(\tilde{h}, \tilde{\mu}_1), \dots, \cos(\tilde{h}, \tilde{\mu}_K)]^\top \in \mathbb{R}^K. \quad (1)$$

Although $\mathcal{P}(h)$ uses the compact model embedding, its axes come entirely from the teacher. The projection therefore positions the example within a teacher-defined semantic layout without requiring teacher forward passes.

3.4 Discretization Into Control Tokens

The projection vector is continuous. Each component is discretized into one of B bins:

$$z_i = \text{Quantize}(\mathcal{P}(h)_i), \quad z_i \in \{0, \dots, B-1\}.$$

Each bin index is mapped to a control token:

$$t_i = \text{Token}(z_i).$$

The prefix $[t_1, \dots, t_K]$ encodes coarse manifold coordinates and enters through the model’s input embedding layer, distributing geometric signals throughout the network.

3.5 Training-Time Input Conditioning

For each training example:

1. Compute the intermediate embedding $h = f_\theta^{(\text{emb})}(x)$.
2. Project using $\mathcal{P}(h)$.
3. Discretize and map bins to tokens, forming $[t_1, \dots, t_K]$.
4. Form the new input $x' = [t, x]$.
5. Train with $\mathcal{L}(x'; \theta)$.

The projection and discretization steps are detached from the gradient graph, so no gradients flow into anchors or token assignment.

3.6 Variants of ECR

Global smoothing. Uses all K anchors for projection, yielding globally smooth manifold coordinates.

Retrieval-guided. For finer control, retrieve the k nearest anchors:

$$\mathcal{R}(h) = \arg \underset{\mu_j}{\text{top-k}} \cos(\tilde{h}, \tilde{\mu}_j).$$

3.7 Computational Considerations

ECR adds modest overhead:

- Projection: $O(Kd)$.
- Token quantization: $O(K)$.
- No additional gradients or parameters.
- Inference uses one projection step per query; decoding is unchanged.

3.8 Limitations and Extensions

ECR provides lightweight geometric cues, but with limits:

- Anchor quality constrains the available signal.
- Discretization trades expressiveness for token budget.
- ECR shapes geometry only through input conditioning.

Its simplicity keeps it compatible with common compression methods, since it introduces no auxiliary losses or routing components.

4 Motivation and Design Principles

ECR is motivated by the observation that compact multilingual students struggle not because they fail to match teacher logits, but because the semantic structure of a large teacher cannot be faithfully represented in a constrained embedding space. Building on the geometric perspective introduced in Section 3.1, we examine three hypotheses that link manifold quality to downstream behavior.

Geometry Distortion Hypothesis. When a high capacity multilingual teacher is compressed into a sub-billion-parameter student, the resulting representation space tends to lose local neighborhood structure. Previously distinct regions become closer or overlap, and relative distances become less reliable. We expect this degradation to manifest as increased within-region variance and reduced separation between semantic regions.

Manifold Smoothing Hypothesis. ECR introduces coarse geometric coordinates through projection-based control tokens. If these signals help the compact models remain in more capacity-compatible regions of its manifold, we expect to observe: (i) reduced variance within each semantic region, (ii) clearer boundaries between regions, and (iii) improved preservation of relative structure compared to KD alone.

Functional Consistency Hypothesis. If the embedding geometry becomes more coherent under ECR, the model’s functional outputs should also become more stable. In particular, we anticipate: (i) lower training NLL, (ii) more consistent cross-lingual responses, (iii) more stable retrieval behavior, even if the student–teacher cosine similarity does not necessarily increase. This reflects the view that improvements

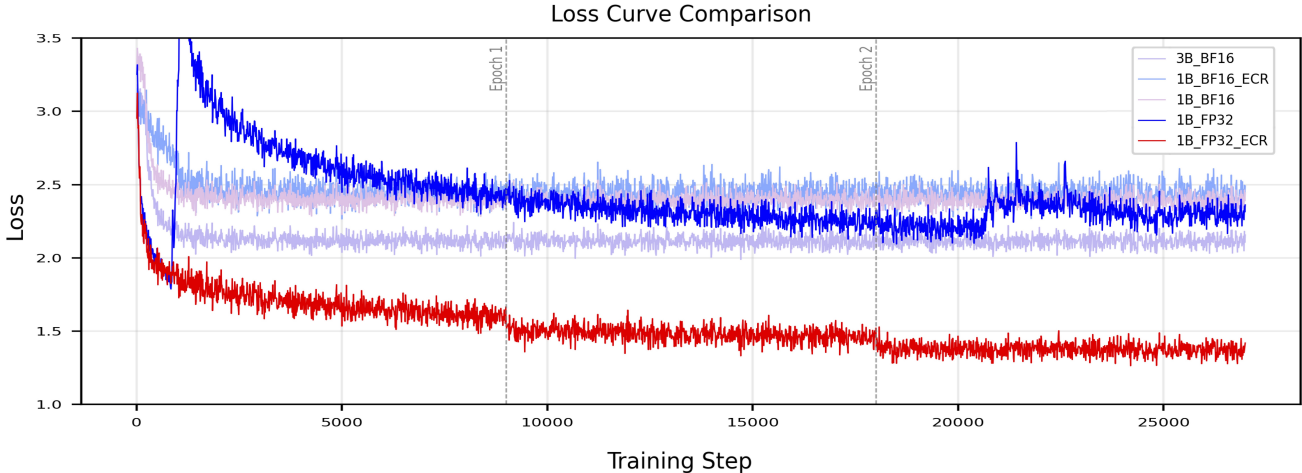


Figure 3: Training loss curves for all configurations. FP32 models converge normally at the beginning, but without ECR the baseline cannot remain stable and its loss eventually explodes under the no-gradient-clipping setting. In contrast, the 1B FP32+ECR model stays stable throughout. The 3B BF16 model also converges, but its multi-task training signal makes it less steady than the 1B FP32+ECR run. Dashed lines mark epoch boundaries.

arise from preserving usable structure rather than matching pointwise activations.

Together, these hypotheses link ECR’s geometric formulation with the experimental observations reported in later sections.

5 Evaluation

We evaluate ECR in a multilingual training setup. The compact models, which differ in size, are trained on the same synthetic instruction–response corpus generated by a high-capacity cloud LLM.

Our aim is to see whether ECR helps smaller models narrow the performance and geometric gaps created by capacity differences. We use the 3B model, trained without ECR, as the higher-capacity baseline for evaluating stability and representation quality in smaller multilingual models.

This setup makes the capacity mismatch evident. It is most pronounced in multilingual data, especially across distant languages like English, Chinese, and Hindi. This makes it a good setting for evaluating whether ECR smooths the induced manifold.

We begin by describing the dataset and model setup, followed by the metrics used in evaluation. We then present quantitative results, geometric analyses, and ablation and cross-lingual studies.

5.1 Dataset

In many practical, real-world settings, language models work with private and domain-specific data. This is especially common in customer-service, finance, healthcare, and government applications. Such data is tightly access-controlled and generally cannot be shared across institutions due to privacy and

Table 1: Dataset statistics.

Language	Train	Test	Avg. Length
English	30k	3.4k	124.6
Chinese	30k	3.3k	138.0
Hindi	30k	3.3k	172.2
Total	90k	10k	144.9

compliance regulations. As a result, open-domain corpora do not reflect the closed-domain conditions under which compact on-device models are actually deployed.

In situations where data cannot be shared, synthetic corpora are widely used. We follow this practice and use a teacher-generated multilingual dataset that matches the structure of domain-restricted tasks. This lets us test ECR in the multilingual settings it is intended to handle, under tight capacity and privacy constraints.

The dataset contains English, Chinese, and Hindi instruction–response pairs. All student models are trained on the same corpus. Table 1 summarizes the dataset statistics.

5.2 Model Configurations

We evaluate two compact model capacities that reflect realistic on-device deployment budgets. All models follow a decoder-only Transformer architecture compatible with the Llama-3.2 family and share the same tokenizer, vocabulary, and special token definitions.

- **3B baseline:** a higher-capacity KD-trained student without ECR, used as the reference system.
- **1B:** the main evaluation model, compared under KD-only and KD+ECR settings.

Aside from the use of ECR, all training and architectural components remain identical across models.

Architectural Details. The **1B** model contains 16 decoder blocks with a hidden size of 2048, **32 attention heads** (head dimension 64), and an MLP dimension of 8192.

The **3B** model contains 28 decoder blocks with a hidden size of 3072, **24 attention heads** (head dimension 128), and an MLP dimension of 8192.

They follow the same architectural conventions—GQA with 8 key-value heads, RMSNorm, RoPE with long-context scaling, and tied embeddings—so the only difference between them is their capacity.

5.3 Training Setup

All models are trained for three epochs on the 100k multilingual instruction-response corpus. During training, we use a per-device batch size of 10, and a gradient accumulation factor of 1. We use AdamW with a learning rate of 1×10^{-6} , linear decay, and 200 warmup steps. A padding token is added to the tokenizer, and the embedding matrix is resized accordingly.

Two precision settings are considered. By default, all students are trained in BF16 with FlashAttention-2 and gradient checkpointing enabled. For precision analysis, the 1B model and its ECR variant are additionally trained in FP32, which uses the standard attention implementation.

ECR shapes the input rather than the loss, so it brings in no additional objectives or tuning weights. Other than capacity and the use of ECR, the training setup is identical across runs.

Optimization Hyperparameters. We use AdamW with $\beta_1 = 0.9$, $\beta_2 = 0.95$, $\epsilon = 10^{-8}$, and weight decay of 0.1. All models employ identical optimization parameters, initialization, tokenization, batching strategy, and training schedule to ensure a controlled comparison.

No Gradient Clipping (Strict-Control Setting). To examine the *natural gradient dynamics* of ECR, we disable gradient clipping (`max_grad_norm = 0`) for *all* models. LLM fine-tuning usually relies on gradient clipping. Otherwise, gradients may spike during training. With clipping removed for every model, any remaining stability differences reflect the model’s own behavior.

As shown in Fig. 3, without gradient clipping, the FP32 run collapses early, but FP32+ECR continues normally. This suggests that ECR keeps the FP32 dynamics from blowing up.

On several specific tasks, we notice a consistent trend. The 1B+ECR model settles into its stable range earlier than the 3B baseline. This happens even though the 3B model has more capacity. These cases suggest that ECR offers smaller models a cleaner and more efficient starting point.

5.4 Evaluation Metrics

We evaluate ECR with five metrics:

Table 2: Negative log-likelihood (NLL). Lower is better. ECR yields substantial improvements, especially under FP32.

Model	English	Chinese	Hindi
3B (BF16)	2.94	3.04	2.30
1B BF16	3.14	3.33	2.49
1B BF16 + ECR	3.44	3.59	2.75
1B FP32	3.59	3.50	2.76
1B FP32 + ECR	2.76	2.79	2.12

5.4.1 Embedding Alignment Score

Cosine similarity between teacher and student embeddings.

5.4.2 Retrieval Consistency

Agreement between teacher and student in selecting semantic manifolds.

5.4.3 Generation Coherence

KL divergence, semantic similarity (SemSim), and answer-level faithfulness.

5.4.4 Cross-Lingual Consistency

Probability that aligned English/Chinese/Hindi variants activate the same manifold subset.

5.4.5 Task Accuracy

Accuracy on the small classification questions baked into the corpus.

5.5 Main Quantitative Results

Table 2 reports NLL for the three languages. Two main trends appear.

The 1B BF16 and 1B FP32 baselines land above the 3B KD-only model on NLL. This is consistent with the capacity difference. Under FP32, the 1B model drops to 2.76 (English), 2.79 (Chinese), and 2.12 (Hindi). These scores outperform the 3B baseline on all three languages. This suggests that once the manifold is better organized, the capacity gap matters less. In some cases, a smaller model can even outperform a larger one.

5.6 Teacher Similarity

Table 3 presents cosine similarity between teacher and student embeddings. Interestingly, ECR slightly lowers teacher similarity. This behavior is expected: ECR regularizes the *student* manifold rather than enforcing pointwise embedding matching. Despite minor decreases in similarity, both generation quality and manifold structure improve substantially, as shown later. The result points to one thing. Geometry matters more than local alignment in compact multilingual models.

Table 3: Teacher–student embedding similarity (cosine). Higher is better. ECR maintains alignment while improving geometry.

Model	English	Chinese	Hindi
3B BF16	0.746	0.867	0.930
1B BF16	0.801	0.852	0.922
1B BF16 + ECR	0.789	0.855	0.902
1B FP32	0.785	0.867	0.906
1B FP32 + ECR	0.762	0.840	0.902

Table 4: Representation geometry (lower intra, higher inter, lower ratio are better). ECR significantly improves manifold structure.

Model	Intra \downarrow	Inter \uparrow	Ratio \downarrow
3B BF16	42.51	43.54	0.976
1B BF16	48.02	48.95	0.981
1B BF16 + ECR	41.17	42.48	0.969
1B FP32	46.51	47.33	0.983
1B FP32 + ECR	39.66	41.91	0.946

5.7 Representation Geometry

Table 4 summarizes intra-manifold compactness, inter-manifold separation, and their ratio. ECR improves every geometric indicator across both BF16 and FP32. The improvement is most pronounced in FP32, where 1B FP32+ECR attains the lowest intra-manifold variance (39.66), the highest inter-manifold separation (41.91), and the lowest ratio (0.946), outperforming even the 3B teacher.

These structural improvements correlate with the observed NLL reductions in Table 2, indicating that more coherent manifold organization improves the ease of optimization in compact multilingual models.

5.8 Stability Without Gradient Clipping

Multilingual LLM training almost universally employs gradient clipping to suppress gradient spikes arising from high-curvature teacher manifolds. Surprisingly, the FP32 student *without* ECR diverges in the first epoch under the no-clipping setup. The FP32+ECR run stays stable under the same conditions.

This suggests a simpler explanation: the ECR-shaped manifold avoids the extreme updates that normally cause FP32 to blow up when clipping is off. The stability comes from better representational coherence. It does not rely on changing the gradients or the objective.

5.9 Language Manifold Coherence

To verify that languages indeed form coherent semantic submanifolds, we compute language-specific prototype centers using the 1B student embeddings. For each language $\ell \in \{\text{En, Zh, Hi}\}$, we average sentence embeddings to obtain a language prototype μ_ℓ . Given a test embedding $h(x)$ with label ℓ , we compute its distances to all prototypes. The assigned label

Table 5: Ablation over manifold subsets. Lower NLL and Spread are better.

Manifolds	NLL \downarrow	Consistency (Sim) \uparrow	Spread \downarrow
None (KD only)	2.655	0.863	55.428
L (Label-only)	2.715	0.863	54.610
E (Emotion)	2.867	0.859	52.485
I (Intent)	2.873	0.859	52.393
E+I	2.881	0.859	52.117
L+I	2.874	0.859	52.002
E+I (alt)	2.915	0.852	50.717
All (L+E+I)	2.943	0.852	50.288

$\hat{\ell}$ is the nearest center:

$$\hat{\ell} = \arg \min_{\ell'} \|h(x) - \mu_{\ell'}\|_2.$$

We define language manifold purity as the fraction of sentences with $\hat{\ell} = \ell$. The purity remains high on 200 mixed-language sentences. English is 0.82, Chinese is 0.76, and Hindi is 0.75. These values show that each language occupies its own part of the embedding space. They do not collapse into a single region. This empirical behavior supports our treatment of language as a semantic manifold and justifies the language-aware geometric regularization employed by ECR.

5.10 Cross-Lingual Consistency

Because each Chinese seed produces aligned English–Chinese–Hindi variants, we measure whether a model assigns these triplets to the same semantic manifolds. ECR improves cross-lingual manifold consistency across all languages. The largest gain appears in Hindi, which has the biggest typological gap and the highest teacher-manifold curvature. The result points to a simple pattern: ECR lowers cross-lingual curvature and brings the language submanifolds together in a cleaner way.

5.11 Ablation Study

We ablate two components of ECR:

1. the choice of semantic manifolds used to construct anchors,
2. the discretization budget, which controls how many control tokens are inserted (i.e., the number of bins or anchor dimensions used in quantization).

Because ablation models are trained on only 10% of the data for a single epoch, these experiments highlight the *early-stage behavior* of ECR. Even in this short regime, ECR immediately improves geometric structure—reducing embedding dispersion and tightening cross-lingual neighborhoods—while having minimal influence on short-horizon NLL. This delayed-benefit pattern is consistent with manifold-based methods observed in prior work.

Interpretation. Across manifold subsets and discretization budgets, ECR consistently reduces Spread, indicating

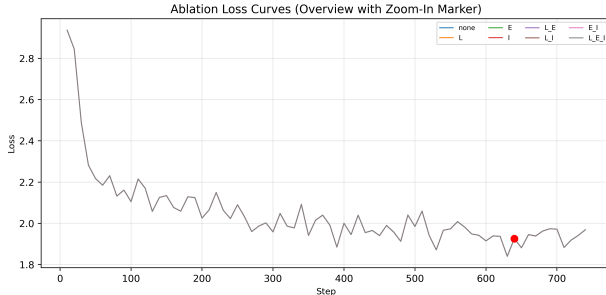


Figure 4: Ablation loss curves (overview). All manifold subsets exhibit nearly identical optimization behavior during the first epoch, indicating that ECR does not destabilize training even under aggressive regularization settings. The highlighted point corresponds to the region magnified in Fig. 5.

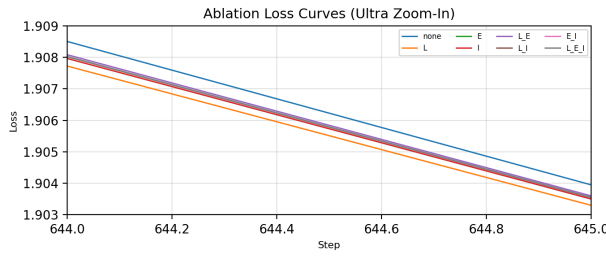


Figure 5: Ultra-zoom-in view of the ablation loss curves around step 644–645. All curves remain nearly perfectly parallel, confirming that geometric regularization affects manifold structure without perturbing the local optimization dynamics.

smoother manifolds and tighter cross-lingual neighborhoods. Although NLL may increase slightly during the earliest training steps due to the introduction of additional control tokens, the geometric improvements reliably predict the later-stage NLL gains observed in Table 2. This confirms that ECR primarily influences representational geometry through input conditioning, rather than manipulating gradients or modifying the loss.

5.12 Summary of Findings

Across three languages, two precision formats, and multiple student capacities, we observe consistent improvements when the proposed regularizer is applied:

- **NLL decreases substantially** under full convergence, with the strongest gains in FP32 (Table 2).
- **Representation geometry improves immediately**, with tighter neighborhoods and clearer separation between semantic regions.
- **Cross-lingual stability increases** across English, Chinese, and Hindi.
- **1B students approach or match the 3B KD-only baseline**, demonstrating the ability of ECR to close capacity gaps.

Table 6: Ablation over discretization budget. A higher budget corresponds to more control tokens. Lower NLL and Spread are better.

Token Budget	NLL ↓	Spread ↓	Consistency ↑
Small	2.655	55.428	0.863
Medium	2.881	52.117	0.859
Large	2.943	50.288	0.852

These findings support the hypothesis that smoothing the embedding manifold is more effective than relying solely on pointwise KD signals. The results further confirm that multilingual capacity–distribution mismatch—not optimization difficulty—is the dominant bottleneck in compact multilingual training.

6 Conclusion

We introduce *Embedding Consistency Regulation*(ECR), a manifold-level regularization method. It helps compact models match large multilingual models despite the capacity–distribution gap. Traditional compression methods focus on local signals such as logits or hidden states. But these signals do not shape the global geometry of the representation space. ECR keeps related embeddings together and aligns their cross-lingual versions.

This leads to steadier training and less drift between languages. It also produces cleaner representation geometry and lower NLL in English, Chinese, and Hindi. The strongest gains occur in the low-capacity models. This supports the view that geometric mismatch, rather than optimization difficulty, limits compact multilingual training.

Overall, the results show that manifold-level regularization fills a gap left by standard compression methods. It also scales well and helps small multilingual models keep the structure of their teachers.

7 Discussion

a) *Geometric Control vs. Conventional Compression.* Traditional distillation puts most of the pressure on the hidden layers. compact models must normally identify the task and intent before they can respond, which consumes limited attention budget. ECR’s control tokens shape the embedding right from the start. They guide it into the manifold region that corresponds to the intended task. The student no longer spends capacity deciding what the task is. It can focus on doing the task instead. This shift is what allows compact models to behave more reliably under multilingual or resource-limited conditions.

b) *What ECR Does Not Address.* ECR depends on having a well-defined semantic manifold. Its control signals work best when the task space is narrow and the labels are clean. When the domain becomes too broad, the projection becomes less precise. Noisy data makes this worse, and the control tokens begin to drift. ECR is not built for open-ended dialogue or

unconstrained semantic space. It works best when the task and the domain have a stable structure it can anchor to.

c) *Precision and Robustness*. Full precision keeps the manifold stable enough for ECR to guide it. BF16 introduces early noise that breaks this structure and limits how much ECR can influence the geometry.

d) *Deployment Settings*. ECR works well when predictable behavior is needed under tight budgets. Many finance, healthcare, and government applications run fully on-device and operate under strict memory and compute limits. In these situations, ECR helps keep each task steady and the model's behavior consistent.

8 Future Work

ECR suggests several directions beyond single-turn language modeling. A natural next step is to move from single-turn control to handling full conversations. ECR keeps each turn reasonably well-formed, but compact models still drift once they start conditioning on their own earlier outputs. In practice, even a simple rewriting step for the most recent turns can help. This gives the model a small amount of usable state instead of letting the noise accumulate.

A second line of work focuses on understanding the underlying mechanism. Although the experiments show clear differences between FP32 and BF16, it is still not clear how far geometric signals travel through the network or where they fade out. Simple teacher–student setups or stability tests may shed light on the question.

Finally, ECR aligns well with on-device systems. Future designs may combine ECR with quantization-aware training. Small retrieval modules or compact summarizers could be added as well. These pieces can form a local pipeline for tasks like translation or secure enterprise workflows. Domain-specific geometric cues could help even more in settings where all computation stays on-device.

References

[1] Xubin Wang, Zhiqing Tang, Jianxiong Guo, Tianhui Meng, Chenhao Wang, Tian Wang, and Weijia Jia. Empowering edge intelligence: A comprehensive survey on on-device ai models. *arXiv:2503.06027v2*, 2025.

[2] Paul Voigt and Axel von dem Bussche. *The EU General Data Protection Regulation (GDPR): A Practical Guide*. Springer, Cham, Switzerland, 2017. doi:10.1007/978-3-319-57959-7.

[3] Sina Shaham, Arash Hajisafi, Minh K. Quan, Dinh C. Nguyen, Bhaskar Krishnamachari, Charith Peris, Gabriel Ghinita, Cyrus Shahabi, and Pubudu N. Pathirana. Privacy and fairness in machine learning: A survey. *IEEE Transactions on Artificial Intelligence*, 6(7):1706–1728, 2025. doi:10.1109/TAI.2025.3531326.

[4] Muhammad Fahim, S. M. Ahsan Kazmi, Vishal Sharma, Hyundong Shin, and Trung Q. Duong. Edge intelligence: A deep distilled model for wearables to enable proactive eldercare. *IEEE Transactions on Artificial Intelligence*, 6(7):1736–1745, 2025. doi:10.1109/TAI.2025.3527400.

[5] Z. Liu, C. Zhao, F. Iandola, C. Lai, Y. Tian, I. Fedorov, Y. Xiong, E. Chang, Y. Shi, R. Krishnamoorthi, L. Lai, and V. Chandra. Mobilellm: Optimizing sub-billion parameter language models for on-device use cases. *arXiv:2402.14905*, 2024. doi:10.48550/arXiv.2402.14905.

[6] Keivan Alizadeh, Iman Mirzadeh, Dmitry Belenko, Karen Khatamifard, Minsik Cho, Carlo C. Del Mundo, Mohammad Rastegari, and Mehrdad Farajtabar. Llm in a flash: Efficient large language model inference with limited memory. *arXiv preprint arXiv:2312.11514*, 2024. doi:10.48550/arXiv.2312.11514. ACL 2024.

[7] Jianping Gou, Baosheng Yu, Stephen J. Maybank, and Dacheng Tao. Knowledge distillation: A survey. *International Journal of Computer Vision*, 129(6):1789–1819, 2021.

[8] Geoffrey Hinton, Oriol Vinyals, and Jeff Dean. Distilling the knowledge in a neural network. *arXiv:1503.02531*, 2015.

[9] Siqi Sun, Yu Cheng, Zhe Gan, and Jingjing Liu. Patient knowledge distillation for BERT model compression. In *Proceedings of the 2019 Conference on Empirical Methods in Natural Language Processing*, pages 4314–4323, Hong Kong, China, 2019. Association for Computational Linguistics. doi:10.18653/v1/D19-1441.

[10] Junjie Yang, Junhao Song, Xudong Han, Ziqian Bi, Tianyang Wang, Chia Xin Liang, Xinyuan Song, Yichao Zhang, Qian Niu, Benji Peng, Keyu Chen, and Ming Liu. Feature alignment and representation transfer in knowledge distillation for large language models. *arXiv:2504.13825*, Apr 2025.

[11] Qitong Wang, Mohammed J. Zaki, Georgios Kollias, and Vasileios Kalantzikis. Multi-sense embeddings for language models and knowledge distillation. *arXiv:2504.06036*, Apr 2025. 16 pages, 4 figures. Computation and Language (cs.CL).

[12] David E. Rumelhart and James L. McClelland. Chapter 3: Distributed representations. In *Parallel Distributed Processing: Explorations in the Microstructure of Cognition: Foundations*, pages 75–109. MIT Press, 1987.

[13] Yoshua Bengio, Aaron Courville, and Pascal Vincent. Representation learning: A review and new perspectives. *IEEE Transactions on Pattern Analysis and Machine Intelligence*, 35(8):1798–1828, 2013. doi:10.1109/TPAMI.2013.50.

[14] Aaron van den Oord, Yazhe Li, and Oriol Vinyals. Representation learning with contrastive predictive coding. *arXiv:1807.03748*, 2018. doi:10.48550/arXiv.1807.03748.

[15] Sam T Roweis and Lawrence K Saul. Nonlinear dimensionality reduction by locally linear embedding. *Science*, 290(5500):2323–2326, 2000.

[16] Joshua B Tenenbaum, Vin De Silva, and John C Langford. A global geometric framework for nonlinear dimensionality reduction. *Science*, 290(5500):2319–2323, 2000.

[17] Mikhail Belkin and Partha Niyogi. Laplacian eigenmaps for dimensionality reduction and data representation. In *Neural Information Processing Systems*, pages 585–591, 2003.

[18] Michael M. Bronstein, Joan Bruna, Yann LeCun, Arthur Szlam, and Pierre Vandergheynst. Geometric deep learning: Going beyond euclidean data. *IEEE Signal Processing Magazine*, 34(4):18–42, 2017. doi:10.1109/MSP.2017.2693418.

[19] C. Bucilua, R. Caruana, and A. Niculescu-Mizil. Model compression. In *Proceedings of the 12th ACM SIGKDD International Conference on Knowledge Discovery and Data Mining (KDD)*, pages 535–541, 2006. doi:10.1145/1150402.1150464.

[20] Wenhui Wang, Furu Wei, Li Dong, Hangbo Bao, Nan Yang, and Ming Zhou. Minilm: Deep self-attention distillation for task-agnostic compression of pre-trained transformers. *arXiv:2002.10957*, 2020. doi:10.48550/arXiv.2002.10957.

[21] Xiaoqi Jiao, Yichun Yin, Lifeng Shang, Xin Jiang, Xiao Chen, Linlin Li, Fang Wang, and Qun Liu. Tinybert: Distilling BERT for natural language understanding. In *Proceedings of the 2020 Conference on Empirical Methods in Natural Language Processing (EMNLP)*, pages 4163–4174, Online, 2020. Association for Computational Linguistics. doi:10.18653/v1/2020.emnlp-main.372.

[22] Yonglong Tian, Dilip Krishnan, and Phillip Isola. Contrastive representation distillation. In *International Conference on Learning Representations (ICLR)*, 2020.

[23] Zhiwei Hao, Jianyuan Guo, Ding Jia, Kai Han, Yehui Tang, Chao Zhang, Han Hu, and Yunhe Wang. Learning efficient vision transformers via fine-grained manifold distillation. *arXiv:2107.00374*, 2021. Version 4, last revised 2 Jun 2022.

[24] Patrick Lewis, Ethan Perez, Aleksandra Piktus, Fabio Petroni, Vladimir Karpukhin, Naman Goyal, Heinrich Küttler, Mike Lewis, Wen-tau Yih, Tim Rocktäschel, et al. Retrieval-augmented generation for knowledge-intensive nlp tasks. *Advances in Neural Information Processing Systems*, 33:9459–9474, 2020.

[25] Shitao Xiao, Zheng Liu, Yingxia Shao, and Zhao Cao. Retromae: Pre-training retrieval-oriented language models via masked auto-encoder. In *Proceedings of the 2022 Conference on Empirical Methods in Natural Language Processing*, pages 538–548, Abu Dhabi, United Arab Emirates, 2022. Association for Computational Linguistics. doi:10.18653/v1/2022.emnlp-main.35.

[26] Sebastian Borgeaud, Arthur Mensch, Jordan Hoffmann, Trevor Cai, Eliza Rutherford, Katie Millican, George van den Driessche, Jean-Baptiste Lespiau, Bogdan Damoc, Aidan Clark, Diego de Las Casas, Aurelia Guy, Jacob Menick, Roman Ring, Tom Hennigan, Saffron Huang, Loren Maggiore, Chris Jones, Albin Cassirer, Andy Brock, Michela Paganini, Geoffrey Irving, Oriol Vinyals, Simon Osindero, Karen Simonyan, Jack W. Rae, Erich Elsen, and Laurent Sifre. Improving language models by retrieving from trillions of tokens. *arXiv:2112.04426*, 2022.

[27] Jason Wei, Xuezhi Wang, Dale Schuurmans, Maarten Bosma, Brian Ichter, Fei Xia, Ed Chi, Quoc V. Le, and Denny Zhou. Chain-of-thought prompting elicits reasoning in large language models. In *NeurIPS*, 2022.

[28] Xuezhi Wang, Jason Wei, Dale Schuurmans, Quoc Le, Ed Chi, Sharan Narang, Aakanksha Chowdhery, and Denny Zhou. Self-consistency improves chain-of-thought reasoning in language models. *arXiv*, 2022.

[29] Qiguang Chen, Libo Qin, Jinhao Liu, Dengyun Peng, Jiannan Guan, Peng Wang, Mengkang Hu, Yuhang Zhou, Te Gao, and Wanxiang Che. Towards reasoning era: A survey of long chain-of-thought for reasoning large language models. *arXiv*, 2025.

[30] Yuxiang Gu, Xu Han, Zhiyuan Liu, and Minlie Huang. Ppt: Pre-trained prompt tuning for few-shot learning. In *Proceedings of the 60th Annual Meeting of the Association for Computational Linguistics (ACL)*, pages 8410–8423, 2022.

[31] Xiang Lisa Li and Percy Liang. Prefix-tuning: Optimizing continuous prompts for generation. *arXiv:2101.00190*, 2021. doi:10.48550/arXiv.2101.00190.

[32] David E. Rumelhart and James L. McClelland. Chapter 8: Learning internal representations by error propagation. In *Parallel Distributed Processing: Explorations in the Microstructure of Cognition: Foundations*, pages 318–362. MIT Press, 1987.

Table 7: Field definitions for all training samples.

Field	Description
dialog_id	Unique identifier
task	Primary task label
language	Primary language label
emotion	Primary emotion label
intent	Primary intent label
EN_Q	English query (synthetic)
ZH_Q	Chinese query (synthetic)
HI_Q	Hindi query (synthetic)
EN_A	English answer (teacher-generated)
ZH_A	Chinese answer (teacher-generated)
HI_A	Hindi answer (teacher-generated)

Table 8: On-device runtime configuration and resource usage.

Device	iPhone 14 (iOS 26)
Backend	11ama.cpp with Metal acceleration
Model Format	GGUF (Q4_KM)
Runtime Footprint	693 MB (model + RAG index + runtime)
Peak RAM Usage	1.27 GB
Throughput	14–15 tokens/s (offline)

A Dataset Schema

The training corpus is synthetic and contains multilingual instruction–response pairs generated by a high-capacity teacher model. No real user data is involved. We release the full data schema but not the raw text, which preserves privacy while still enabling reproducibility.

All samples follow this structure. The EN, ZH, and HI versions are aligned in meaning to support cross-lingual training and testing. The semantic labels (emotion and intent) support finegrained supervision for compact-model training.

Preprocessing includes:

- multilingual token normalization,
- OCR corruption injection for robustness,
- label extraction and formatting into the above schema,
- shared tokenizer usage across all models.

The schema is enough to show how the data is processed without exposing any of the original text.

B On-Device Deployment Details

We evaluate the distilled student model in a fully on-device setting. All measurements were collected directly from a physical iPhone 14 during offline inference.

Table 9: Local retrieval subsystem specifications.

Index Type	HNSW, 64-d embeddings
Index Size	48.9 MB
RAG Records	381,943 text entries
Query Latency	< 2 ms/query
Top-k	5
Similarity Metric	Cosine distance

Table 10: Summary of the Luna on-device system.

Model Name	Luna-0.6B
Application Package Size	693 MB
Training Set Size	875,596 dialogue fragments
iPhone Throughput	~15 tokens/s
Core Abilities	summarization, translation, sentiment analysis, offline RAG
Future Work	semantic alignment, ECR extensions

B.1 Hardware and Runtime Configuration

The footprint includes the quantized model, runtime binaries, and the local vector-store database used for retrieval-augmented generation.

B.2 Local Retrieval Subsystem

The device maintains a fully local retrieval pipeline with no external communication. Table 9 summarizes the retrieval subsystem.

C System Overview

Luna is the on-device system that uses ECR to demonstrate practical deployment. It is an application of the proposed prefix mechanism.

Luna runs as a small on-device model with a local retrieval index. The app bundle contains the quantized weights. It also includes the index and a small runtime layer that keeps everything offline. All computation is carried out on the device with no network calls.

ECR functions as a simple prefix layer that decides whether the model should consult the local store or generate directly. The system uses this mechanism to decide when to retrieve. Luna can then handle daily tasks like translation, brief summaries, sentiment cues, and simple lookups.

This appendix summarizes the deployment setup only. All core experiments and analyses remain within the main paper.

D Reproducibility Statement

- All device-level performance measurements were collected on a physical iPhone 14 using the runtime configuration described in Appendix A.
- Dataset statistics and preprocessing procedures correspond to the formats outlined in Appendix B.

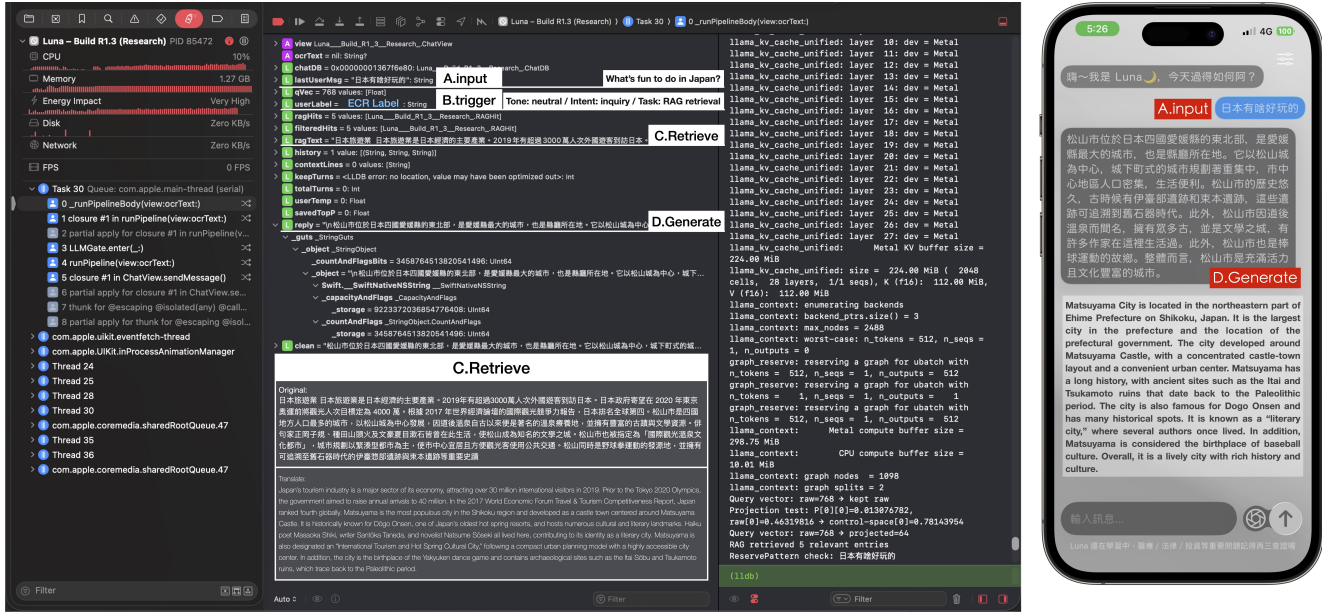


Figure 6: Full Xcode runtime trace from iPhone 14 during on-device inference. The screenshot includes the call stack, KV-cache operations, and the unified attention kernel dumps.

- Due to double-blind review requirements and proprietary components in our deployment stack, implementation artifacts cannot be released during the review period.
- We describe the full training setup and evaluation procedure in the paper. These details are sufficient for others to reproduce our results.

E End-to-End Execution Flow

Fig. 6 illustrates the full inference pipeline running on an iPhone 14. For clarity, the trace is annotated with four stages that correspond to the ECR-aware execution path.

(A) Input Normalization and Embedding. We normalized and tokenized user text with the shared multilingual tokenizer. The tokens are then embedded to form the initial hidden states used by the model.

(B) ECR Geometric Control Prefix. ECR projects the embedding onto its semantic anchors and retrieves the corresponding control tokens as prefix. The prefix contains the fields shown in the trace—Label, Script, Tone (neutral), Intent (inquiry), and Task (RAG retrieve). These values set up the initial embedding path. They also control whether retrieval fires, which is why the trace branches.

(C) Local Retrieval. In the example shown in the figure, the task is RAG retrieve. When the prefix signals retrieval, the system runs a local vector-store search. It returns the entries that fall in the same semantic region. The trace shows the projection to 64 dimensions, cosine scoring, and HNSW top- k selection.

(D) ECR-Stabilized Quantized Decoding. Decoding uses Metal-accelerated Q4_KM GGUF weights. This shows KV-cache reads, attention matvecs, command-buffer calls, and sampling. ECR reduces noise in the embedding updates. This helps the quantized model stay stable while decoding. The full output is produced on-device with no remote computation.